ELSEVIER

Inorganica Chimica Acta 240 (1995) 465–478

Inorganica Chimica Acta

Synthesis and reactions of trigonal-bipyramidal rhenium and technetium complexes with a tripodal, tetradentate NS_3 ligand ☆

Hartmut Spies [a,*], Matthias Glaser [a], Hans-Jürgen Pietzsch [a], F. Ekkehardt Hahn [b,*], Thomas Lügger [b]

[a] *Forschungszentrum Rossendorf e. V., Institut für Bioanorganische und Radiopharmazeutische Chemie, PO Box 510 119, 01217 Dresden, Germany*
[b] *Institut für Anorganische und Analytische Chemie, Freie Universität Berlin, 14195 Berlin, Germany*

Received 2 March 1995; revised 16 June 1995

Abstract

Neutral, trigonal-bipyramidal complexes of technetium and rhenium with the tripodal, tetradentate ligand 2,2',2''-nitrilotris(ethanethiol), $N(CH_2CH_2SH)_3$ (H_3**1**) have been synthesized and characterized. The technetium complex [^{99}Tc(**1**)(PPh_3)] (**2**) can be obtained by reduction of $K^{99}TcO_4$ with PPh_3 in the presence of H_3**1** or by substitution reaction starting from [$^{99}TcCl_3(PPh_3)_2(NCMe)$]. The trigonal-bipyramidal complex **2**, $C_{24}H_{27}NPS_3Tc$, crystallizes in the monoclinic space group $P2_1/c$ with $a=8.906(2)$, $b=25.804(6)$, $c=11.061(4)$ Å, $\beta=108.42(2)°$ and $Z=4$. Rhenium complexes [Re(**1**)(PR_3)] (**3**) ($PR_3=PPh_3$ (**3a**), PMe_2Ph (**3b**), $PMePh_2$ (**3c**), P(n-Bu)$_3$ (**3d**), P(OEt)$_3$ (**3e**)) have been obtained in analogy to the technetium derivative **2** by reduction of NH_4ReO_4 with phosphines PR_3 in the presence of H_3**1**. Complex **3a**, $C_{24}H_{27}NPReS_3$, crystallizes in the monoclinic space group $P2_1/n$ with $a=10.855(3)$, $b=16.707(4)$, $c=15.441(5)$ Å, $\beta=92.62(2)°$ and $Z=4$. Rhenium complexes containing an isocyanide co-ligand [Re(**1**)(CNR)] (**5**) (R=CH_2COOMe (**5a**), t-Bu (**5b**), Ph (**5c**), $CH_2CH_2NC_4H_8O$ (**5d**), CH_2COOEt (**5e**)) can be prepared by substitution of the phosphine ligand in **3** for an isocyanide or by reaction of the isocyanide complexes [$ReCl_3(PPh_3)_2(CNR)$] (**4**) (R=CH_2COOMe (**4a**), t-Bu (**4b**), Ph (**4c**), $CH_2CH_2NC_4H_8O$ (**4d**)) with H_3**1**. The crystal structure of complex **4b** has been determined. **4b** crystallizes with one molecule of CH_2Cl_2 per formula unit. Crystals of **4b**·CH_2Cl_2, $C_{42}H_{41}Cl_5NP_2Re$, are monoclinic, space group $P2_1/c$ with $a=12.868(3)$, $b=20.454(7)$, $c=16.378(9)$ Å, $\beta=104.71(4)°$ and $Z=4$. The substitution reaction starting with complexes of type **3** gives the best yields in the preparation of complexes of type **5**. Two complexes of the type [Re(**1**)(CNR)] were characterized by X-ray crystallography. Crystals of **5a**, $C_{10}H_{17}N_2O_2ReS_3$, are monoclinic, space group $P2_1/c$ with $a=7.827(4)$, $b=13.866(3)$, $c=13.627(6)$ Å, $\beta=93.19(7)°$ and $Z=4$. Crystals of **5b**, $C_{11}H_{21}N_2ReS_3$, are monoclinic, space group $P2_1/c$ with $a=12.084(2)$, $b=11.915(2)$, $c=12.244(3)$ Å, $\beta=114.31(2)°$ and $Z=4$. Treatment of **5e** with LiOH leads to ester hydrolysis and yields the complex [Re(**1**)($CNCH_2COOH$)] (**6**) while reaction of **5b–5e** in the two-phase system toluene/conc. hydrochloric acid gives the carbonyl complex [Re(**1**)(CO)] (**7**) which was characterized by X-ray crystallography. Crystals of **7**, $C_7H_{12}NOReS_3$, are triclinic, space group $P\bar{1}$ with $a=7.924(2)$, $b=10.467(3)$, $c=13.556(2)$ Å, $\alpha=96.61(2)$, $\beta=90.47(2)$, $\gamma=101.68(2)°$ and $Z=4$ (2 molecules of **7** per asymmetric unit).

Keywords: Crystal structures; Rhenium complexes; Technetium complexes; Trigonal-bipyramidal complexes; Isocyanide complexes

1. Introduction

Only a few trigonal-bipyramidal technetium and rhenium complexes containing ligands with sulfur donor-atoms are known [1–3]. In a preliminary communication we reported recently the syntheses and molecular structures of some trigonal-bipyramidal Re(III) and Tc(III) complexes with the tripodal, tetradentate ligand $N(CH_2CH_2SH)_3$ (H_3**1**) and a monodentate coligand [4]. In these complexes, the coordinated ligand **1** enforces a trigonal-bipyramidal coordination geometry. Our interest in such complexes is based on the application of ^{99m}Tc and ^{186}Re in radiodiagnosis and radiotherapy, respectively [5]. Technetium and rhenium complexes, which are suitable for coupling to biologically relevant molecules are particularly interesting for the design of new radiopharmaceuticals. To date most technetium or rhenium compounds suitable for coupling, are tetragonal-pyramidal complexes of the oxo ions $M{=}O^{3+}$ with tetradentate ligands [5–7]. However, the properties and thus the in vivo behavior of such complexes are influenced by the polar M=O unit. In this contribution we present trigonal-bipyr-

☆ This paper is dedicated to Professor Fred Basolo on the occasion of his 75th birthday.

* Corresponding authors.

SSDI 0020-1693(95)04571-P

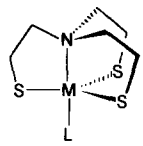

M = Tc(III), L = PPh_3, **2**
M = Re(III), L = PR_3, **3**
M = Re(III), L = CNR, **5**
M = Re(III), L = $CNCH_2COOH$, **6**
M = Re(I), L = CO, **7**

Fig. 1. Trigonal-bipyramidal complexes of technetium and rhenium with the tetradentate ligand **1** and a monodentate coligand.

amidal complexes (see Fig. 1), which are neutral and less polar since they contain sterically well shielded, oxo-free M(III) ions. Coupling of these complexes to molecules with a specific biodistribution can be achieved by (i) substitution of the monodentate coligand L or (ii) reaction at the coligand. For example, ester substituted isocyanides in complexes of type **5** could be used for coupling of the complex to a primary amine via formation of an amide bond. In addition, a neutral complex of type **5**, in which the isocyanide ligand is substituted with an ester group can be converted into an anionic derivative of type **6** via ester hydrolysis and deprotonation of the formed carboxylic acid. Such behavior can influence the in vivo biodistribution of the complex. Technetium complexes with hydrolyzable ester groups are currently under investigation as cerebral perfusion imaging agents [5]. Neutral complexes with ester substituted ligands have been shown to be able to cross the blood-brain-barrier where the ester substituent undergoes enzymatic hydrolysis to give the carboxylic acid (or the deprotonated anion), which is sufficient to trap the complex in the brain, since the now charged species is unable to diffuse back across the blood-brain-barrier.

2. Experimental

2.1. Methods and materials

The phosphines used in this study were purchased from Merck. Isocyanides were obtained from Alpha Products (for **4b/5b**) and Merck (for **4d/5d**). Phenylisocyanide (for **4c/5c**), methylisocyanacetate (for **4a/5a**) and ethylisocyanacetate (for **5e**) were prepared as described in the literature [8]. $[ReCl_3(PPh_3)_2(NCMe)]$ was prepared by reduction of $[Re(O)Cl_3(PPh_3)_2]$ [9] with an excess of triphenylphosphine [10]. $[^{99}TcCl_3(PPh_3)_2(NCMe)]$ was prepared from commercial $K^{99}TcO_4$ according to the method published by Davison and co-workers [11]. All manipulations were performed in an atmosphere of dry argon or nitrogen using standard Schlenk techniques. Solvents were dried by standard methods und freshly distilled prior to use. IR spectra were measured as KBr pellets on a Carl Zeiss Specord M80. Bruker WH 90 and AM 250 spectrometers were used for all ^1H NMR spectra. Elemental analyses were performed on a LECO CHNS 932 Elemental Analyzer at the Institut für Bioanorganische und Radiopharmazeutische Chemie, Forschungszentrum Rossendorf or on a Heraeus CHN-Rapid Elemental Analyzer at the Institut für Anorganische und Analytische Chemie, Freie Universität Berlin.

2.2. Preparation of compounds

2.2.1. $N(CH_2CH_2SH)_3$ (H_3**1**)

The preparation of H_3**1** was achieved as depicted in Scheme 1 [4a]. The tris(thioacetate) was synthesized by refluxing 5.0 g (20.7 mmol) of tris(2-chloroethyl)amin hydrochloride and 12.0 g (105 mmol) of potassium thioacetate in 100 ml of ethanol for 5 h. After the solvents were removed the residue was dissolved in a solution made from 1.2 g of KOH and 20 ml of water. The water solution was extracted three times with diethyl ether (50 ml for each extraction) and the combined ether extracts were dried with Na_2SO_4. Removal of the ether solvent gave 5.9 g (88%) of the tris(thioacetate) as a yellow oil. ^1H NMR (250 MHz, $CDCl_3$): δ 2.36 (s, 9H, CH_3), 2.72 (t, 6H, NCH_2), 2.96 (t, 6H, SCH_2). ^{13}C NMR (63 MHz, $CDCl_3$): δ 27.32 (H_2CS), 30.59 (CH_3), 53.18 (NCH_2), 195.81 (C=O).

For the synthesis of H_3**1** 2.1 g (6.5 mmol) tris(thioacetate) were dissolved in 15 ml of dry THF. This solution was added dropwise over 10 min to a suspension of 1.0 g (28.6 mmol) of $LiAlH_4$ in 40 ml of dry THF at 0 °C. After the addition was complete, the reaction mixture was stirred for an additional 12 h at r.t. Then 2.2 ml of degassed water were added slowly and insoluble material was separated by filtration. All solvents were removed and the residue was suspended in 40 ml of dry THF which was saturated with CO_2. The solution was again filtered. After removal of the solvent, H_3**1** was obtained as a yellow oil. Yield: 0.67 g (52%). *Anal.* Found: C, 36.52; H, 7.27; N, 7.62. Calc. for $C_6H_{15}NS_3$: C, 36.51; H, 7.66; N, 7.10%. ^1H NMR (250 MHz,$CDCl_3$): δ 1.80 (s, 3H, SH), 2.72 (m, 12, NCH_2 and SCH_2). ^{13}C NMR (63 MHz, $CDCl_3$): δ 22.81 (H_2CS), 57.01 (NCH_2). IR (KBr): ν(SH) 2543 cm^{-1}.

2.2.2. Synthesis of $[^{99}Tc(1)(PPh_3)_2]$ (2)

Complex **2** was prepared by a reduction/substitution reaction from $K^{99}TcO_4$ (method A) or by a substitution route from $[^{99}TcCl_3(PPh_3)_2(NCMe)]$ (method B) according to Scheme 2 [4a].

Method A. 66 mg (0.250 mmol) PPh_3 and 20 mg (0.101 mmol) of H_3**1** were dissolved in 3 ml of ethanol. This solution was added to a solution of 20 mg (0.100 mmol) $KTcO_4$ in 2 ml of water/ethanol (2:1 (vol./vol.)). The reaction mixture was acidified with three drops of acetic acid and was stirred at r.t. for 5 h. During this time a black–violet solid precipitated. The solid was filtered off and extracted three times with 1 ml of benzene. Addition of 1 ml of methanol to the combined violet benzene extracts and subsequent slow evaporation of the solvents gave 31 mg (56% rel. to $K^{99}TcO_4$) violet needles of **2**.

Method B. 9 mg (0.046 mol) of H_3**1** were dissolved in 1 ml of methanol. To this solution were added 31 mg (0.046 mmol) of $[^{99}TcCl_3(PPh_3)_2(NCMe)]$ [11] dissolved in 2 ml of dichloromethane. Upon mixing of the solutions, the colour changed from orange–brown to violet. After a few minutes a black solid began to precipitate. The reaction mix-

ture was stirred for 1 h at r.t. The precipitate was separated by filtration and was extracted three times with 1 ml of benzene. Addition of 1 ml methanol to the benzene extracts and evaporation of most of the solvents in a nitrogen stream overnight gave 14.7 mg (66% rel. to [$^{99}TcCl_3(PPh_3)_2(NCMe)$]) of violet crystals of **2** suitable for X-ray structure analysis. Both methods yield identical **2** characterized by elemental analysis, ^1H NMR spectroscopy (Table 1) and crystal structure analysis.

2.2.3. *Syntheses of complexes [Re(1)(PR$_3$)] (3a–e)*

The synthetic procedure for the preparation of complexes **3a–e** was very similar (Scheme 3) [4a]. Here we describe the synthesis of **3b** in detail. A sample of 100 mg (0.37 mmol) NH_4ReO_4 and 0.35 ml of conc. HCl (37%) were dissolved in 100 ml of ethanol. This solution was vigorously stirred while H_3**1** (0.063 ml, 0.446 mmol, dissolved in a mixture of 1 ml acetone and 25 ml ethanol) and 0.265 ml of $P(CH_3)_2(C_6H_5)$ (1.86 mmol, dissolved in 25 ml ethanol) were added dropwise and simultanously. After complete addition the reaction mixture was refluxed for 7.5 h. Solvents were stripped in vacuo and the complex was purified by column chromatorgraphy (column 15×250 mm, stationary phase silica 0.04–0.063 mm, eluent $CHCl_3$/acetone, 12:1 (vol./vol.)). Yield: 116.8 mg (61%). **3a–3e** were prepared in a similar fashion. It should be noted that the formation of **3e** from NH_4ReO_4, H_3**1** and $P(OEt)_3$ does not require addition of hydrochloric acid, although the yield is low (14%). Yields, analytical and spectroscopic data for **3a–3e** are summarized in Table 1.

2.2.4. *Syntheses of [ReCl$_3$(PPh$_3$)$_2$(CNR)] (4a-d)*

Similar reaction conditions were employed for the preparation of **4a–d** (Scheme 4) [12] from [$ReCl_3(PPh_3)_2(NCMe)$]. In a typical reaction 200 mg (0.233 mmol) of the Re(III) precursor were dissolved in 10 ml of dry benzene in a nitrogen atmosphere. 0.350 mmol of the isocyanide were added under nitrogen und the reaction mixture was refluxed for 30 min. Then the volume was reduced under nitrogen. This led normally to precipitation of the yellow complexes **4**. If no precpitation was observed after volume reduction, the reaction mixture was taken to dryness and the solid residue was dissolved in 2 ml of dichloromethane. Crystallization was then induced by addition of 5 ml of ethanol. The solid raw material was washed with diethyl ether. Recrystallization from dichloromethane/ethanol gave the yellow, crystalline complexes **3a–e** in 70–80% yield. The preparation of complexes of type **4** is also possible in a one-pot synthesis starting from [$Re(O)Cl_3(PPh_3)_2$]. The yield for this reduction/substitution reaction is generally lower (sometimes as low as 3–5%) than for the reaction starting with the Re(III) precursor. Additional experimental details for the preparation of complexes of type **4** and spectral data for **4a–4d** are summarized in Ref. [12].

2.2.5. *Syntheses of [Re(1)(CNR)] (5a–5e)*

Two synthetic routes leading to complexes of type **5** were explored (Scheme 5) [4a]. The best yields were obtained with complexes of type **3** as starting material (method A). Complexes of type **5** can also be obtained in lower yield from reactions starting with complexes of type **4** (method B).

Table 1
Analytical and physical data for the complexes **2** and **3a–3e**

Complex	Formula	Yield (%)	Elemental analysis (%) [a]				M.p. (°C)	^1H NMR (90 MHz, $CDCl_3$)			
			C	H	N	S		δ (ppm)	Mult.	Int.	Assign.
2a	$C_{24}H_{27}NPS_3Tc$	66	51.48	4.76	2.71	16.95	169 (decomp.)	3.0	m	12H	SCH_2 and NCH_2
		method B	(51.97)	(4.91)	(2.53)	(17.34)		7.3	m	15H	Ar–H
3a	$C_{24}H_{27}NPS_3Re$	57	44.74	4.31	2.19	14.73	234 (decomp.)	2.9	m	12H	SCH_2 and NCH_2
			(44.84)	(4.23)	(2.18)	(14.97)		7.2	m	15H	Ar–H
3b	$C_{14}H_{23}NPS_3Re$	61	32.23	4.23	2.38	18.99	212 (decomp.)	2.12	d	6H	CH_3
			(32.42)	(4.47)	(2.70)	(18.54)		2.87	m	12H	SCH_2 and NCH_2
								7.55	m	5H	Ar–H
3c	$C_{19}H_{25}NPS_3Re$	52	39.16	4.14	2.14	17.02	213 (decomp.)	2.41	d	3H	CH_3
			(39.29)	(4.34)	(2.41)	(16.56)		2.98	m	12H	SCH_2 and NCH_2
								7.50	m	10H	Ar–H
3d	$C_{18}H_{39}NPS_3Re$	36	36.53	6.27	2.81	17.09	210 (decomp.)	0.91	m	9H	CH_3
			(37.09)	(6.74)	(2.40)	(16.50)		1.43	m	12H	CH_2–CH_2
								1.86	m	6H	P–CH_2
								2.82	m	12H	SCH_2 and NCH_2
3e	$C_{12}H_{27}NS_3O_3PRe$	14	26.65	4.98	2.69	17.15	221 (decomp.)	1.31	t	9H	CH_3
			(26.36)	(4.98)	(2.56)	(17.59)		2.92	m	12H	SCH_2 and NCH_2
								4.00	q	6H	O–CH_2

[a] Calculated values are in parentheses.

Table 2
Analytical and physical data for the complexes **5a–5e**, **6** and **7**

Complex	Formula	Yield (%)	Elemental analysis (%) [a]				M.p. (°C)	^{1}H NMR (90 MHz, $CDCl_3$)				IR (KBr) ν (cm^{-1})
			C	H	N	S		δ (ppm)	Mult.	Int.	Assign.	
5a	$C_{10}H_{17}N_2O_2S_3Re$	86 method A	25.37 (25.04)	3.56 (3.57)	5.68 (5.84)	19.79 (20.05)	205	3.02 3.81 5.46	m s s	12H 3H 2H	SCH_2 and NCH_2 OCH_3 N-CH_2-C(O)	1940 (CN) 1976 (CN)
5b	$C_{11}H_{21}N_2S_3Re$	64 method A 20 method B (from **4b**)	28.77 (28.49)	4.60 (4.56)	5.86 (6.04)	20.80 (20.74)	238 (decomp.)	1.54 2.98	s m	9H 12H	CH_3 SCH_2 and NCH_2	1976 (CN)
5c	$C_{13}H_{17}N_2S_3Re$	63 method A	32.24 (32.28)	3.53 (3.54)	5.56 (5.79)	20.09 (19.89)	206	3.08 7.19	m m	12H 5H	SCH_2 and NCH_2 Ar–H	1842 (CN)
5d	$C_{13}H_{24}N_3OS_3Re$	81 method A	30.28 (29.98)	4.43 (4.65)	7.79 (8.07)	18.62 (18.47)	184	2.61 2.81 2.98 3.73 4.88	m t m m t	4H 2H 12H 4H 2H	morpholine NCH_2 NCH_2 SCH_2 and NCH_2 morpholine OCH_2 CN-CH_2	1968 (CN)
5e	$C_{11}H_{19}N_2O_2S_3Re$	90 method A	26.83 (26.76)	3.77 (3.88)	5.46 (5.67)	19.97 (19.48)	170	1.31 3.02 4.28 5.45	t m q s	3H 12H 2H 2H	CH_3 SCH_2 and NCH_2 OCH_2 CN-CH_2	1976 (CN) 1741 (CO)
6	$C_9H_{15}N_2O_2S_3Re$	58	23.33 (23.22)	3.38 (3.25)	5.96 (6.02)	20.18 (20.66)	197 (decomp.)	2.88 5.37	m s	12H 2H	SCH_2 and NCH_2 CN–CH_2	1924 (CN) 1720 (CO)
7	$C_7H_{12}NOS_3Re$	64 (from **5e**) 42 (from **5d**) 37 (from **5b**) <5 (from **5c**)	20.56 (20.58)	2.70 (2.86)	3.24 (3.43)	24.31 (23.54)	280	3.12	m	12H	SCH_2 and NCH_2	1876 (CO)

[a] Calculated values are in parentheses.

Method A will be illustrated with the synthesis of **5b**. 100 mg (0.156 mmol) of [Re(**1**)(PPh_3)] (**3a**) were dissolved in 5 ml of dichloromethane. At r.t. 0.024 ml (0.233 mmol, dissolved in 2.5 ml of dichloromethane) of t-butylisocyanide were added dropwise over 10 min. After the addition was complete, TLC showed the presence of **5b** and of unreacted **3a**. The product **5b** was isolated by column chromatography (column 15×250 mm, stationary phase silica 0.063–0.10 mm, eluent CH_2Cl_2). Sometimes it was neccessary to wash the isolated complex of type **5** with diethyl ether to remove traces of unreacted isocyanide. Analytical and spectroscopic data for complexes of type **5** are summarized in Table 2. Method B for the synthesis of **5b**: 0.100 mg (0.104 mmol) of **4b**·CH_2Cl_2 were dissolved in 100 ml of acetone. To this solution were added 0.047 ml (0.152 mmol, dissolved in 2 ml of acetone) of H_3**1**. The yellow colour of the solution changed to green upon addition of the ligand H_3**1**. The reaction mixture was refluxed for 30 min. Workup was carried out as described for method A. However, the yield was normally only up to 20%.

2.2.6. Synthesis of [Re(1)(CNCH$_2$COOH)] (6)

For the synthesis of **6** (Scheme 6) 50 mg (0.101 mmol) of **5e** were dissolved in 5 ml of THF. To this solution were added 7 mg of LiOH·H_2O (0.167 mmol, dissolved in 0.5 ml water). The reaction mixture was stirred for 1 h at r.t. and then the THF was removed by a nitrogen stream. 10 ml of cation exchange resin suspension (DOWEX 50 WX8) were added to the remaining aqueous phase. After stirring for 2 h, complex **6** was extracted with acetonitrile (4×2 ml). Recrystallization from acetonitrile/water (10:1 (vol./vol.)) gave olive green needles (27.4 mg, 58%) of **6**. Analytical and spectroscopic data for **6** can be found in Table 2.

2.2.7. Synthesis of [Re(1)(CO)] (7)

50 mg (0.101 mmol) of **5e** were dissolved in a mixture of dichloromethane (1 ml) and toluene (10 ml). To this solution was added under nitrogen 1 ml of conc. hydrochloric acid (37%). The mixture was heated under reflux for 2 h. During the first hour the original green colour of the organic phase bleached and the water phase turned orange. Continued heating of the reaction mixture gave a lipophilic compound, which redissolved in the CH_2Cl_2/toluene phase. Finally, the red toluene phase was separated, washed with water (3×2 ml) and dried over Na_2SO_4. Solvents were removed and the residue was dissolved in 1 ml of dichloromethane. Addition of 1 ml of ethanol led to the formation of red crystals of **7** in 64% yield (Table 2). A good yield (42%) under similar conditions was also obtained starting with **5d**. The yield in the reaction with **5b** was only 37% while only traces of **7** could be isolated from the reaction of **5c** with hydrochloric acid (Table 2, Scheme 6).

2.3. X-ray crystallography

Crystals of **2**, **5a**, **5b** and **7** were mounted on glass fibers and data were collected on an Enraf-Nonius CAD-4 four circle diffractometer. **4b** crystallized from CH_2Cl_2/ethanol as CH_2Cl_2 solvate **4b**·CH_2Cl_2. These crystals are sensitive towards loss of CH_2Cl_2. They as well as crystals of the air-sensitive complex **3a**, were mounted directly in the cold stream (−100(2) °C) of an Enraf-Nonius CAD-4 diffractometer using a modified version of the device described by Veith and Bärnighausen [13]. Standard centering and autoindexing procedures indicated monoclinic cells for all but crystals of **7**, which were triclinic. Intensity data were collected at −100(2) °C for **4b**·CH_2Cl_2 and **3a** and at room temperature for all other crystals. Intensity data were converted into structure factors [14]. Empirical absoption corrections based on Ψ-scans were applied to the data for **5b** and **7** while DIFABS [15] was used for absorption corrections for **3a**, **4b**·CH_2Cl_2 and **5a**. No absorption correction was applied to the data for **2**. The systematically absent intensities allowed unambiguous assignment of the space group for all crystals except **7** which was assumed to belong to space group $P\bar{1}$. This choice proved to be correct by the successful solution and refinement of the structure of **7**. All structures were solved by Patterson methods and refined by full matrix least-squares. All hydrogen atoms were added to the models on calculated positions (d(C–H) = 0.95 Å) [16]. Calculations were carried out with the MolEN package of programs [14]. Neutral atomic scattering factors were taken from Ref. [17] and the scattering factors for non-hydrogen atoms were corrected for anomalous dispersion [18]. Crystals of **3a** appeared to decompose in the X-ray beam. Therefore only a small data set ($5.4 \leq 2\theta \leq 40°$) could be collected. To maintain a reasonable rate of the number of reflections to the number of refined parameters, only positional parameters of the heavy atoms Re, S and P were refined with anisotropic thermal parameters. The asymmetric unit of **7** contains two almost identical molecules. Selected data collection and refinement parameters are given in Table 3. Tables 4–9 list positional and equivalent isotropic thermal parameters. Selected bond distances and angles are summarized in Tables 10–13. Additional data concerning the crystal structure determinations are available as supplementary material (see Section 5).

3. Results and discussion

3.1. Ligand synthesis

The synthesis of the tripodal ligand H_3**1** [4a,19] was achieved by reaction of commercial tris(2-chloroethyl)amine hydrochloride with potassium thioacetate followed by reduction with $LiAlH_4$ (Scheme 1). It is com-

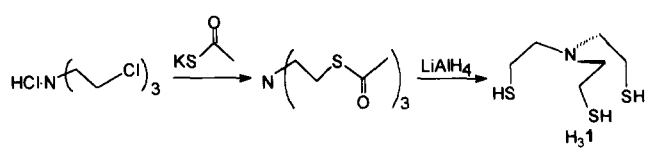

Scheme 1.

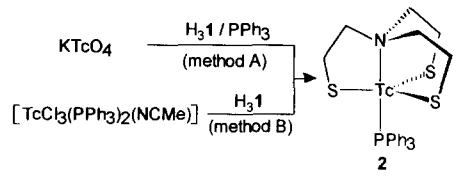

Scheme 2.

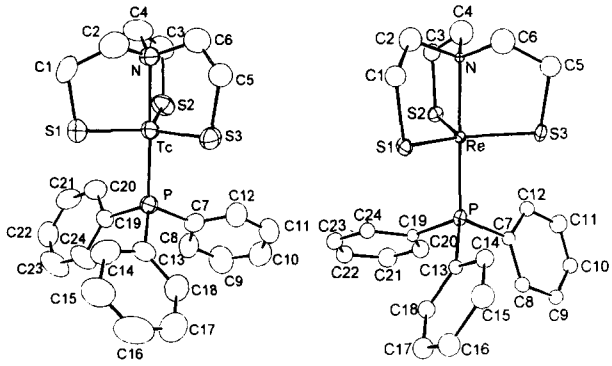

Fig. 2. Molecular structure of **2** (left) and **3a** (right).

plicated by the presence of both acidic (SH) and basic (tertiary amine) functional groups in the same molecule. However, the formation of ionic compounds (hydrochloride or thiolate) can be supressed by introduction of CO_2 during workup. H_3**1** was isolated as yellow oil, which is stable for weeks under argon.

3.2. Technetium complex

The technetium complex **2** can be synthesized from $KTcO_4$ (method A) or from $[TcCl_3(PPh_3)_2(NCMe)]$ (method B) according to Scheme 2. For the reaction starting with $KTcO_4$, triphenylphosphine was added as a reducing agent and the reaction was carried out in an acidified solution. The yield in this reaction is slightly lower, than in the synthesis of **2** from the Tc(III) precursor $[TcCl_3(PPh_3)_2(NCMe)]$. Complex **2** adopts the rare trigonal-bipyramidal molecular structure as shown by X-ray crystallography (Fig. 2). Ligand **1** occupies one axial (N) and three equatorial (S) positions of the trigonal bipyramid. The ligand constitutes the second example of an 'umbrella' ligand, a concept introduced by Davison and co-workers [2]. The 'umbrella' in Davison's complexes consists of a central phosphorus atom and three aromatic thiolate functions (PS_3), while in **2** three aliphatic thiolates and a central nitrogen atom form the 'umbrella' ligand **1** (NS_3). These differences, however, do not lead to large differences in the Tc–S bond distances (Table 10). Only the Tc–N distance in **2** is slightly shorter than the Tc–P distance in Davison's complexes [2b]. All N–Tc–S angles in **2** are smaller than 90° and fall in the same range as the P–Tc–S angles in trigonal-bipyramidal Tc complexes with the PS_3 ligand. Based on the crystal structure data, it appeares, that the space requirements of the NS_3 ligand in **2** and the PS_3 ligand in Davison's complexes are about the same. A triphenylphos-

Table 3
Selected crystal and data collection details

Parameter	**2**	**3a**	**4b**·CH_2Cl_2	**5a**	**5b**	**7**
Crystal size (mm)	0.38×0.20×0.07	0.50×0.35×0.10	0.45×0.40×0.25	0.52×0.48×0.25	0.40×0.35×0.15	0.35×0.25×0.25
Formula	$C_{24}H_{27}NPS_3Tc$	$C_{24}H_{27}NPReS_3$	$C_{42}H_{41}Cl_5NP_2Re$	$C_{10}H_{17}N_2O_2ReS_3$	$C_{11}H_{21}N_2ReS_3$	$C_7H_{12}NOReS_3$
Formula weight (a.m.u.)	554.66	642.86	985.21	479.65	463.70	408.57
a (Å)	8.906(2)	10.855(3)	12.868(3)	7.827(4)	12.084(2)	7.924(2)
b (Å)	25.804(6)	16.707(4)	20.454(7)	13.866(3)	11.915(2)	10.467(3)
c (Å)	11.061(4)	15.441(5)	16.378(9)	13.627(6)	12.244(3)	13.556(2)
α (°)	90.0	90.0	90.0	90.0	90.0	96.61(2)
β (°)	108.42(2)	92.62(2)	104.71(4)	93.19(7)	114.31(2)	90.47(2)
γ (°)	90.0	90.0	90.0	90.0	90.0	101.68(2)
V (Å^3)	2412(2)	2797(2)	4169(5)	1476(2)	1606.6(12)	1093.2(9)
Space group	$P2_1/c$	$P2_1/n$	$P2_1/c$	$P2_1/c$	$P2_1/c$	$P\bar{1}$
Z	4	4	4	4	4	4
D_{calc} (g cm^{-3})	1.527	1.526	1.569	2.157	1.917	2.482
D_{obs} (g cm^{-3})	1.53	1.53	1.58	2.17	1.93	2.50
μ (Mo Kα) (cm^{-1})	9.1	46.8	33.8	87.4	80.26	117.82
Data collection T (°C)	20(2)	−100(2)	−100(2)	20(2)	20(2)	20(2)
2θ Range (°)	$2 \le 2\theta \le 50$	$5.4 \le 2\theta \le 40$	$2 \le 2\theta \le 50$	$2 \le 2\theta \le 50$	$2 \le 2\theta \le 50$	$2 \le 2\theta \le 45$
hkl Range	$0 \le h \le 10$	$-10 \le h \le 10$	$0 \le h \le 13$	$0 \le h \le 9$	$0 \le h \le 14$	$0 \le h \le 8$
	$0 \le k \le 30$	$-16 \le k \le 0$	$0 \le k \le 24$	$0 \le k \le 16$	$0 \le k \le 14$	$-11 \le k \le 11$
	$-12 \le l \le 12$	$0 \le l \le 14$	$-18 \le l \le 18$	$-16 \le l \le 16$	$-13 \le l \le 13$	$-14 \le l \le 14$
No. unique data	4233	2592	7340	2589	2822	2863
No. observed data $F_o^2 \ge 3\sigma(F_o^2)$	2410	1824	6190	2350	2425	2543
R [a]	0.0373	0.0651	0.0429	0.0410	0.0462	0.0250
R_w [a]	0.0456	0.0893	0.0727	0.0609	0.0655	0.0371
GOF	1.022	1.682	1.667	1.433	1.501	1.001
No. variables	271	147	446	163	155	236

[a] $R = \Sigma\Delta F/\Sigma F_o$, $R_w = [\Sigma w \Delta F^2/\Sigma F_o^2]^{1/2}$, $GOF = [\Sigma w||F_o| - |F_c||^2/(n_o - n_p)]^{1/2}$.

Table 4
Positional and equivalent isotropic thermal parameters for **2** [a]

Atom	x	y	z	B_{eq} (Å^2)
Tc	0.49286(6)	0.07430(2)	0.74638(5)	2.382(8)
S1	0.4113(2)	0.08764(7)	0.91459(15)	3.67(4)
S2	0.6716(2)	0.01293(7)	0.7556(2)	3.79(4)
S3	0.3534(2)	0.10578(6)	0.55670(14)	3.16(4)
P	0.6729(2)	0.14241(6)	0.79639(13)	2.40(3)
N	0.3200(6)	0.0110(2)	0.7016(4)	3.0(1)
C1	0.2550(8)	0.0393(3)	0.8946(6)	4.8(2)
C2	0.1916(9)	0.0220(3)	0.7564(8)	5.6(2)
C3	0.5550(9)	−0.0463(3)	0.7283(6)	4.5(2)
C4	0.3985(10)	−0.0383(3)	0.7549(8)	6.0(2)
C5	0.1997(8)	0.0566(3)	0.4963(6)	3.8(2)
C6	0.2478(9)	0.0053(3)	0.5610(7)	5.7(2)
C7	0.8088(7)	0.1497(2)	0.7021(5)	2.9(1)
C8	0.9670(7)	0.1621(3)	0.7547(6)	3.8(2)
C9	1.0600(8)	0.1711(3)	0.6776(7)	5.3(2)
C10	0.9962(8)	0.1696(3)	0.5475(6)	4.5(2)
C11	0.8398(8)	0.1566(3)	0.4946(6)	4.4(2)
C12	0.7479(7)	0.1461(3)	0.5702(6)	4.0(2)
C13	0.5839(7)	0.2073(2)	0.7832(5)	2.8(1)
C14	0.4830(8)	0.2180(3)	0.8528(7)	4.3(2)
C15	0.4143(8)	0.2665(3)	0.8468(8)	5.4(2)
C16	0.4400(9)	0.3030(3)	0.7670(8)	5.7(2)
C17	0.5389(11)	0.2933(3)	0.6985(7)	6.2(2)
C18	0.6101(9)	0.2457(3)	0.7062(6)	4.8(2)
C19	0.8127(6)	0.1433(2)	0.9590(5)	2.5(1)
C20	0.8832(8)	0.0970(3)	1.0108(6)	3.7(2)
C21	0.9958(8)	0.0960(3)	1.1300(7)	4.4(2)
C22	1.0371(8)	0.1397(3)	1.2014(6)	4.5(2)
C23	0.9684(10)	0.1857(3)	1.1507(7)	5.9(2)
C24	0.8578(9)	0.1876(3)	1.0303(7)	4.5(2)

[a] E.s.d.s are given in parentheses. The isotropic thermal parameter B_{eq} is defined as $8/3\pi^2[\Sigma_i\Sigma_j U_{ij} a_i^* a_j^* \mathbf{a}_i\mathbf{a}_j]$.

Table 5
Positional and equivalent isotropic thermal parameters for **3a** [a]

Atom	x	y	z	B_{eq} (Å^2)
Re	0.25362(7)	0.04771(6)	0.61818(5)	0.78(2)
S1	0.1117(5)	0.1413(4)	0.6440(4)	1.4(1)
S2	0.1983(5)	−0.0673(4)	0.5554(4)	1.5(1)
S3	0.4534(5)	0.0817(4)	0.6224(4)	1.3(1)
P	0.2569(5)	−0.0014(4)	0.7578(4)	1.1(1)
N	0.2512(15)	0.0979(17)	0.4876(16)	0.5(3)*
C1	0.091(2)	0.1939(15)	0.537(2)	2.0(5)*
C2	0.127(2)	0.135(2)	0.463(2)	2.8(6)*
C3	0.188(2)	−0.0418(15)	0.4407(15)	1.9(5)*
C4	0.263(3)	0.030(2)	0.424(2)	3.6(6)*
C5	0.471(2)	0.127(2)	0.517(2)	2.4(5)*
C6	0.350(2)	0.153(2)	0.477(2)	3.3(6)*
C7	0.394(2)	−0.0580(14)	0.7983(14)	1.1(4)*
C8	0.430(2)	−0.0582(14)	0.8849(14)	1.4(4)*
C9	0.531(2)	−0.1046(14)	0.9140(15)	1.3(5)*
C10	0.587(2)	−0.1514(15)	0.8567(15)	1.5(5)*
C11	0.556(2)	−0.152(2)	0.773(2)	2.4(5)*
C12	0.454(2)	−0.1014(13)	0.7430(15)	1.5(5)*
C13	0.239(2)	0.0769(13)	0.8441(15)	1.0(4)*
C14	0.301(2)	0.1487(15)	0.8327(14)	1.6(5)*
C15	0.287(2)	0.211(2)	0.890(2)	2.4(5)*
C16	0.212(2)	0.199(2)	0.961(2)	2.2(5)*
C17	0.156(2)	0.1301(15)	0.9702(15)	2.0(5)*
C18	0.166(2)	0.0673(14)	0.9129(15)	1.5(5)*
C19	0.134(2)	−0.0701(13)	0.7832(14)	0.9(4)*
C20	0.157(2)	−0.150(2)	0.808(2)	2.2(5)*
C21	0.061(2)	−0.201(2)	0.819(2)	2.8(6)*
C22	−0.062(2)	−0.176(2)	0.809(2)	2.0(5)*
C23	−0.082(2)	−0.0997(15)	0.7842(15)	1.8(5)*
C24	0.011(2)	−0.0497(15)	0.7699(14)	1.5(4)*

[a] E.s.d.s are given in parentheses. The isotropic thermal parameter B_{eq} is defined as $8/3\pi^2[\Sigma_i\Sigma_j U_{ij} a_i^* a_j^* \mathbf{a}_i\mathbf{a}_j]$. Starred atoms were refined with isotropic thermal parameters.

phine is the monodentate coligand in **2**. Our initial report on the possibility to synthesize the hexa-coordinated complex [Tc(**1**)$(PPh_3)_2$] [4a] with two monodentate coligands in the presence of an excess of triphenylphosphine proved irreproducible. This is not surprising in view of the large space requirement of the bulky triphenylphosphine ligand. With the PS_3 ligand and monodentate, sterically less demanding isocyanides, both the trigonal-bipyramidal complex [Tc(PS_3)(CNR)] and the octahedral complex [Tc(PS_3)-$(CNR)_2$] were synthesized and crystallographically characterized [2]. However, the hexa-coordinated species exists only in the presence of a large excess of isocyanide. Tripodal, tetradentate ligands like **1** or PS_3 appear to stabilize Tc(III) in the less common trigonal-bipyramidal coordination geometry even if the complexes are synthesized from octahedral Tc(III) complexes.

3.3. Trigonal-bipyramidal rhenium complexes

Trigonal-bipyramidal complexes of the type [Re(**1**)(PR_3)] **3** can be synthesized in good yield from NH_4ReO_4, H_3**1** and variuos phosphines PR_3 (Scheme 3) which must be present in excess to act as reducing agent and as monodentate complex ligand [4a]. No attempts were made to obtain complexes of type **3** from Re(III) starting materials.

Complexes **3a–3e** are diamagnetic, which allows recording of their ^{1}H NMR spectra (Table 1). The diamagnetism of a Re(III) (d^4) complex indicates that the coordination geometry is not octahedral, since octahedral d^4 complexes cannot be diamagnetic. The X-ray crystal structure analysis of **3a** (Fig. 2) confirms, that indeed a trigonal-bipyramidal complex had been obtained. This complex is, as expected, isostructural to the technetium complex **2**. Again, the tripodal, tetradentate ligand **1** enforces a trigonal-bipyramidal coordination geometry.

Bond distances and angles in **3a** are, within experimental error, identical to those of **2**. This is not surprising, since, for

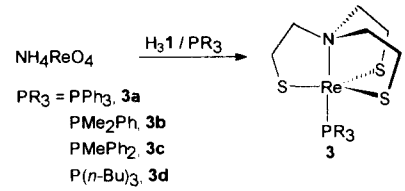

Scheme 3.

Table 6
Positional and equivalent isotropic thermal parameters for **4b**·CH_2Cl_2 [a]

Atom	x	y	z	B_{eq} (Å^2)
Re	0.11527(2)	0.10527(1)	0.19398(1)	1.139(5)
Cl1	0.21481(14)	0.09901(7)	0.33462(10)	2.07(3)
Cl2	0.02274(14)	0.09883(7)	0.05142(9)	1.98(3)
Cl3	0.10425(12)	0.22298(7)	0.20789(9)	1.85(3)
P1	0.28555(13)	0.11964(8)	0.15341(9)	1.43(3)
P2	−0.05471(13)	0.09589(7)	0.23682(9)	1.35(3)
N	0.1498(5)	−0.0466(3)	0.2103(4)	2.5(1)
C1	0.1340(5)	0.0080(3)	0.1996(4)	1.9(1)
C2	0.1808(8)	−0.1121(3)	0.2381(7)	4.4(2)
C3	0.2991(14)	−0.1114(6)	0.2779(11)	10.3(5)
C4	0.1064(9)	−0.1392(5)	0.2805(8)	8.3(3)
C5	0.1836(15)	−0.1526(5)	0.1580(9)	10.6(5)
C6	0.3439(5)	0.0436(3)	0.1259(4)	1.8(1)
C7	0.4494(6)	0.0241(4)	0.1518(5)	3.0(2)
C8	0.4846(6)	−0.0303(4)	0.1230(5)	4.0(2)
C9	0.4191(7)	−0.0664(4)	0.0627(5)	4.1(2)
C10	0.3126(7)	−0.0493(4)	0.0321(5)	3.6(2)
C11	0.2750(6)	0.0058(3)	0.0646(4)	2.5(1)
C12	0.3919(5)	0.1608(3)	0.2326(4)	2.1(1)
C13	0.4102(5)	0.2267(3)	0.2240(4)	2.3(1)
C14	0.4889(6)	0.2583(4)	0.2826(5)	3.4(2)
C15	0.5526(6)	0.2258(4)	0.3485(5)	3.7(2)
C16	0.5368(7)	0.1614(5)	0.3618(5)	4.3(2)
C17	0.4515(6)	0.1277(4)	0.3028(4)	2.9(2)
C18	0.2857(5)	0.1682(3)	0.0599(4)	1.5(1)
C19	0.2074(5)	0.2166(3)	0.0307(4)	2.0(1)
C20	0.2134(6)	0.2546(3)	−0.0380(4)	2.7(1)
C21	0.2970(6)	0.2471(3)	−0.0754(4)	2.4(1)
C22	0.3731(5)	0.1990(3)	−0.0472(4)	2.4(1)
C23	0.3672(5)	0.1607(3)	0.0210(4)	2.0(1)
C24	−0.1139(5)	0.0141(3)	0.2285(4)	2.0(1)
C25	−0.1146(6)	−0.0230(3)	0.1574(4)	2.2(1)
C26	−0.1603(7)	−0.0848(4)	0.1494(5)	3.3(2)
C27	−0.2046(8)	−0.1110(3)	0.2108(6)	3.6(2)
C28	−0.2066(7)	−0.0732(4)	0.2811(5)	4.0(2)
C29	−0.1623(6)	−0.0103(4)	0.2889(4)	2.7(1)
C30	−0.0395(5)	0.1198(3)	0.3475(4)	1.7(1)
C31	0.0118(5)	0.0773(3)	0.4114(4)	2.3(1)
C32	0.0267(6)	0.0959(4)	0.4947(4)	3.0(2)
C33	−0.0065(6)	0.1568(4)	0.5149(4)	3.3(2)
C34	−0.0523(7)	0.1985(4)	0.4525(4)	3.3(2)
C35	−0.0727(6)	0.1796(4)	0.3674(4)	2.5(1)
C36	−0.1689(5)	0.1450(3)	0.1791(4)	1.9(1)
C37	−0.1597(5)	0.1896(3)	0.1181(4)	2.1(1)
C38	−0.2489(6)	0.2256(3)	0.0750(4)	2.5(1)
C39	−0.3461(5)	0.2183(4)	0.0928(5)	2.6(1)
C40	−0.3545(6)	0.1726(4)	0.1568(5)	3.1(2)
C41	−0.2689(5)	0.1374(4)	0.1967(4)	2.6(1)
C42 [b]	0.5629(9)	−0.0338(5)	0.3941(7)	5.8(2)
Cl4 [b]	0.6889(9)	0.0038(6)	0.4684(6)	24.5(4)
Cl5 [b]	0.5470(11)	−0.1149(6)	0.3971(9)	27.7(5)

[a] E.s.d.s are given in parentheses. The isotropic thermal parameter B_{eq} is defined as $8/3\pi^2[\Sigma_i\Sigma_j U_{ij} a_i^* a_j^* \mathbf{a}_i\mathbf{a}_j]$.

[b] C42, Cl4 and Cl5 are the atoms of the CH_2Cl_2 molecule in the asymmetric unit.

Table 7
Positional and equivalent isotropic thermal parameters for **5a** [a]

Atom	x	y	z	B_{eq} (Å^2)
Re1	0.14306(3)	0.19859(2)	0.00689(2)	2.369(7)
S1	0.1322(2)	0.3594(2)	0.00528(13)	4.27(4)
S2	−0.0618(2)	0.11571(13)	−0.07708(12)	3.41(3)
S3	0.3110(2)	0.12395(13)	0.12150(13	3.43(3)
O1	0.5023(7)	0.0181(4)	−0.3408(4)	4.8(1)
O2	0.2775(8)	0.0231(4)	−0.2450(5)	5.9(1)
N1	−0.0445(8)	0.2091(4)	0.1239(4)	3.1(1)
N2	0.4154(10	0.1857(5)	−0.1493(5)	4.9(2)
C1	−0.0196(10)	0.3848(6)	0.0992(6)	4.5(2)
C2	−0.026(2)	0.3058(7)	0.1693(9)	6.4(3)
C3	−0.2365(9)	0.1128(6)	0.0068(6)	4.1(2)
C4	−0.2119(14)	0.1778(10)	0.0869(8)	9.2(3)
C5	0.1790(10)	0.1227(6)	0.2286(5)	4.1(2)
C6	0.0074(13)	0.1453(14)	0.2032(7)	12.6(4)
C7	0.3047(10)	0.1868(5)	−0.0919(6)	3.5(1)
C8	0.4926(9)	0.1444(6)	−0.2314(5)	4.2(2)
C9	0.4092(9)	0.0543(6)	−0.2700(5)	3.9(1)
C10	0.4318(14)	−0.0680(7)	−0.3878(9)	7.1(3)

[a] E.s.d.s are given in parentheses. The isotropic thermal parameter B_{eq} is defined as $8/3\pi^2[\Sigma_i\Sigma_j U_{ij} a_i^* a_j^* \mathbf{a}_i\mathbf{a}_j]$.

Table 8
Positional and equivalent isotropic thermal parameters for **5b** [a]

Atom	x	y	z	B_{eq} (Å^2)
Re	0.18050(2)	0.09275(2)	0.35094(2)	2.597(7)
S1	−0.0041(2)	0.1001(2)	0.2001(2)	3.55(5)
S2	0.3226(2)	0.2183(2)	0.3634(2)	3.90(4)
S3	0.2052(2)	−0.0111(2)	0.5106(2)	3.99(5)
N1	0.1127(6)	0.2250(5)	0.4349(5)	3.5(1)
N2	0.2851(7)	−0.0889(6)	0.2355(8)	5.4(2)
C1	−0.0805(8)	0.2082(8)	0.2512(9)	4.6(2)
C2	0.0107(8)	0.2855(8)	0.3408(9)	4.7(2)
C3	0.2836(8)	0.3402(7)	0.4330(7)	4.0(2)
C4	0.2113(10)	0.3047(8)	0.5026(7)	4.9(2)
C5	0.1543(10)	0.0834(8)	0.5979(8)	5.0(2)
C6	0.0688(9)	0.1713(9)	0.5190(7)	5.2(2)
C7	0.2455(8)	−0.0205(8)	0.2785(7)	4.4(2)
C8	0.3776(7)	−0.1372(8)	0.2055(7)	3.8(2)
C9	0.4250(9)	−0.241(1)	0.2846(10)	6.2(3)
C10	0.4756(11)	−0.0523(12)	0.2263(13)	7.3(4)
C11	0.3220(12)	−0.1684(11)	0.0755(10)	6.7(3)

[a] E.s.d.s are given in parentheses. The isotropic thermal parameter B_{eq} is defined as $8/3\pi^2[\Sigma_i\Sigma_j U_{ij} a_i^* a_j^* \mathbf{a}_i\mathbf{a}_j]$.

example, the ionic radii of penta-coordinated Tc(III) and Re(III) are almost identical [20]. From the microanalytical and spectroscopic data for complexes **3b–3e** it can be concluded, that these complexes also adopt a trigonal-bipyramidal coordination geometry like found in **2** and **3a**.

The most important reaction of complexes of type **3** is the substitution of the monodentate phosphine ligand for another monodentate ligand. We have studied this substitution reaction with isocyanides as monodentate ligand. Complex **3a** reacts with various isocyanides to give isocyanide substituted complexes [Re(**1**)(CNR)] **5** (Scheme 4, method A). Alternatively, complexes of type **5** can be synthesized from Re(III) complexes of type **4**, which contain already the isocyanide ligand [12] and H_3**1** (method B). Method B normally gives poorer yields. Complexes **5a–5e** are diamagnetic

Table 9
Positional and equivalent isotropic thermal parameters for 7 [a]

Atom	x	y	z	B_{eq} (Å^2)
Molecule A				
ReA	0.08923(3)	0.21082(2)	0.21125(2)	2.025(5)
S1A	0.0331(2)	−0.00053(14)	0.23452(11)	2.89(3)
S2A	0.3654(2)	0.30604(15)	0.19279(12)	2.90(3)
S3A	−0.1098(2)	0.33324(15)	0.24364(13)	3.28(3)
O1A	−0.0123(6)	0.1597(5)	−0.0087(3)	4.6(1)
N1A	0.1530(6)	0.2494(4)	0.3736(3)	2.3(1)
C1A	0.0631(8)	0.0078(6)	0.3683(4)	2.9(1)
C2A	0.1901(8)	0.1291(5)	0.4096(4)	2.6(1)
C3A	0.4461(8)	0.3432(6)	0.3211(5)	3.0(1)
C4A	0.3068(8)	0.3581(5)	0.3922(5)	2.9(1)
C5A	−0.0703(8)	0.3861(6)	0.3780(5)	3.5(1)
C6A	0.0013(8)	0.2874(6)	0.4261(4)	3.1(1)
C7A	0.0270(8)	0.1779(6)	0.0745(5)	3.1(1)
Molecule B				
ReB	0.47310(3)	0.78529(2)	0.28732(2)	2.070(5)
S1B	0.5331(2)	0.99732(14)	0.26668(12)	3.03(3)
S2B	0.6964(2)	0.68776(15)	0.30655(12)	2.88(3)
S3B	0.2074(2)	0.6654(2)	0.25186(12)	3.16(3)
O1B	0.3966(7)	0.8339(5)	0.5062(3)	5.0(1)
N1B	0.5159(6)	0.7477(4)	0.1258(3)	2.19(9)
C1B	0.5596(8)	0.9926(6)	0.1324(5)	3.0(1)
C2B	0.6193(8)	0.8715(5)	0.0915(4)	2.7(1)
C3B	0.7582(7)	0.6517(5)	0.1785(5)	2.8(1)
C4B	0.6068(8)	0.6381(5)	0.1059(5)	2.9(1)
C5B	0.2121(8)	0.6161(6)	0.1183(5)	3.2(1)
C6B	0.3441(8)	0.7148(6)	0.0700(5)	3.1(1)
C7B	0.4295(8)	0.8157(6)	0.4230(5)	3.0(1)

[a] E.s.d.s are given in parentheses. The isotropic thermal parameter B_{eq} is defined as $8/3\pi^2[\Sigma_i\Sigma_j U_{ij}a_i^*a_j^*\mathbf{a}_i\mathbf{a}_j]$.

with a trigonal-bipyramidal molecular structure. Two complexes **5a** and **5b** were characterized by X-ray crystallography (Fig. 3). As expected, the ester substituted isocyanide in **5a** is a better π-acceptor than the tert-butylisocyanide in **5b**. This can be seen by the difference in the IR absorption for the C≡N stretching vibration (1940 cm^{-1} for **5a**, 1976 cm^{-1} for **5b**, Table 2). It is also evident in the bond parameters (Table 11). The Re–C7 bond in **5a** (1.905(9) Å) is significantly shorter than the Re–C7 bond in **5b** (1.949(10) Å) and the N2–C7 bond in **5a** is longer than in **5b**. Another indication of strong backbonding from the electron-rich

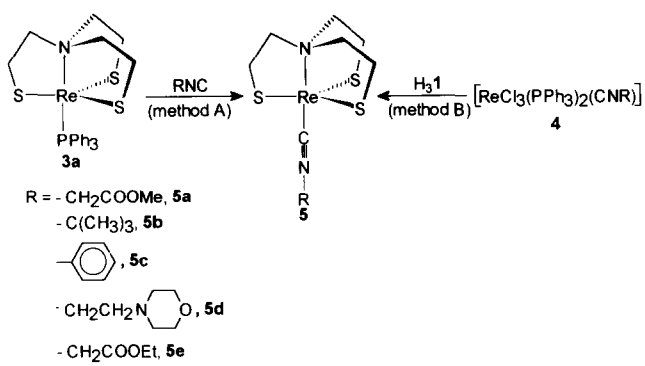

Scheme 4.

Table 10
Selected bond distances (Å) and angels (°) for **2** (M=Tc) and **3a** (M=Re) [a]

	2	**3a**
M–S1	2.228(2)	2.243(6)
M–S2	2.224(2)	2.222(6)
M–S3	2.227(2)	2.240(6)
M–P	2.325(2)	2.306(7)
M–N	2.192(5)	2.18(2)
M–C1	1.829(8)	1.87(3)
M–C3	1.818(8)	1.82(3)
M–C5	1.832(7)	1.82(3)
P–C7	1.841(6)	1.85(2)
P–C13	1.839(6)	1.88(2)
P–C19	1.836(6)	1.82(2)
N–C2	1.482(10)	1.52(3)
N–C4	1.481(10)	1.51(4)
N–C6	1.490(9)	1.43(3)
S1–M–S2	119.29(7)	120.4(2)
S1–M–S3	119.92(7)	119.3(2)
S1–M–P	93.83(6)	93.6(2)
S1–M–N	85.01(2)	85.2(5)
S2–M–S3	118.73(7)	118.3(2)
S2–M–P	95.61(7)	95.3(2)
S2–M–N	85.5(2)	86.4(5)
S3–M–P	94.92(6)	95.1(2)
S3–M–N	85.19(14)	84.3(4)
P–M–N	178.7(2)	178.2(5)
M–S1–C1	103.3(2)	103.1(8)
M–S2–C3	103.2(3)	103.2(8)
M–S3–C5	102.8(2)	102.7(8)
M–P–C7	118.0(2)	118.4(7)
M–P–C13	115.0(2)	114.6(8)
M–P–C19	116.5(2)	116.5(8)
C7–P–C13	101.9(3)	103.0(10)
C7–P–C19	101.0(3)	101.2(10)
C13–P–C19	102.0(3)	101.5(10)
Tc–N–C2	110.0(4)	111.2(14)
Tc–N–C4	109.9(4)	108.4(15)
Tc–N–C6	110.5(4)	112.0(14)
C2–N–C4	109.3(6)	104(2)
C2–N–C6	108.2(6)	112(2)
C4–N–C6	109.0(6)	109(2)

[a] E.s.d.s of the last significant figure are given in parentheses.

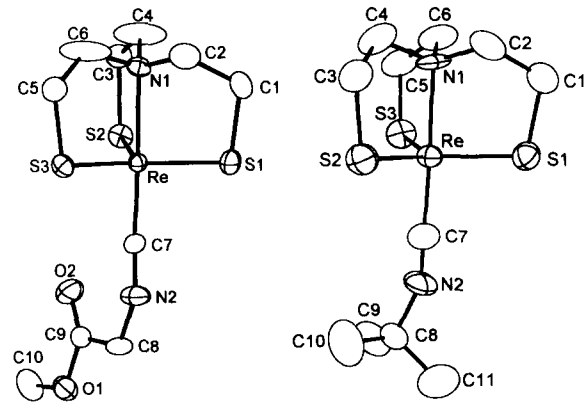

Fig. 3. Molecular structure of **5a** (left) and **5b** (right).

Table 11
Selected bond distances (Å) and angels (°) for **5a** and **5b** [a]

	5a	5b
Re–S1	2.231(2)	2.236(2)
Re–S2	2.235(2)	2.234(2)
Re–S3	2.238(2)	2.227(2)
Re–N1	2.231(7)	2.215(6)
Re–C7	1.905(9)	1.949(10)
S1–C1	1.828(9)	1.837(10)
S2–C3	1.831(8)	1.841(10)
S3–C5	1.834(8)	1.825(11)
O1–C9	1.337(9)	
O1–C10	1.450(13)	
O2–C9	1.185(9)	
N1–C2	1.480(12)	1.482(12)
N1–C4	1.444(14)	1.481(13)
N1–C6	1.437(15)	1.484(12)
N2–C7	1.200(12)	1.174(12)
N2–C8	1.420(11)	1.433(12)
C8–C9	1.492(12)	1.527(15)
C8–C10		1.50(2)
C8–C11		1.50(2)
S1–Re–S2	118.87(8)	120.49(9)
S1–Re–S3	119.31(8)	118.30(9)
S1–Re–N1	85.2(2)	85.5(2)
S1–Re–C7	96.1(2)	95.9(3)
S2–Re–S3	119.74(8)	119.36(9)
S2–Re–N1	85.3(2)	85.0(2)
S2–Re–C7	94.6(3)	93.0(3)
S3–Re–N1	85.2(2)	86.0(2)
S3–Re–C7	93.8(3)	94.7(3)
N1–Re–C7	178.7(3)	177.9(4)
Re–S1–C1	102.2(3)	102.5(3)
Re–S2–C3	103.3(3)	102.9(3)
Re–S3–C5	103.0(3)	102.4(4)
C9–O1–C10	114.7(8)	
Re–N1–C2	107.9(6)	109.5(5)
Re–N1–C4	110.6(6)	110.5(6)
Re–N1–C6	109.1(6)	108.7(6)
C2–N1–C4	118.7(10)	110.1(7)
C2–N1–C6	103.1(12)	109.2(8)
C4–N1–C6	106.9(11)	108.9(7)
C7–N2–C8	150.8(9)	154.0(10)
Re–C7–N2	173.9(8)	179.6(12)
N2–C8–C9	114.7(7)	106.9(9)

[a] E.s.d.s of the last significant figure are given in parentheses.

rhenium atom to the isocyanide carbon atoms is the bond angle at the isocyanide nitrogen atom N2. The stronger the backbonding to the isocyanide carbon atom, the stronger is the sp^2-character at the isocyanide nitrogen atom and the greater is the deviation from linearity for the coordinated isocyanide group. For isocyanide complexes with strong backbonding to the isocyanide carbon atom, C–N–C angles as low as 131(2)° have been observed [21]. For **5a** and **5b** C7–N2–C8 angles of 150.8(9)° and 154.0(10)°, respectively, have been found. The lower value again corresponds to the better π-acceptor in **5a**. We have found no indication for the formation of octahedral diisocyanide substituted complexes, even in the presence of an excess of isocyanide. The $N(S^-)_3$ coordination of Re(III) generates an electron-rich

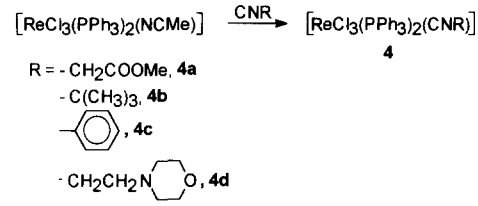

Scheme 5.

transition metal fragment, which engages in strong backbonding to the coordinated isocyanides. This behavior will become important when reactions at the coordinated isocyanide ligand are discussed (vide infra).

Complexes of type **5** can also be synthesized according to method B in Scheme 4. In this synthesis all but the isocyanide ligand in a complex of type **4** are substituted by ligand **1**. Complexes of type **4** are synthesized as shown in Scheme 5 [12]. They are paramagnetic octahedral complexes. Their paramagnetisms can be seen by the unusual chemical shifts for the phenyl protons of the triphenylphosphine ligands [12]. The paramagnetism of octahedral Re(III) (d^4) complexes and its consequences for the ^1H NMR spectra have been discussed [22].

One complex of type **4**, namely **4b**·CH_2Cl_2, was characterized by X-ray structure analysis (Fig. 4). It is interesting to compare the tert-butylisocyanide ligand in the octahedral Re(III) complex **4b**·CH_2Cl_2 with the same ligand in the trigonal-bipyramidal Re(III) complex **5b**. Since **4b**·CH_2Cl_2 is paramagnetic and **5b** is diamagnetic, a comparison of the NMR parameters is worthless. The wavenumbers of the C≡N stretching vibration for **4b**·CH_2Cl_2 (2144 cm^{-1} [12]) and **5b** (1976 cm^{-1}) differ strongly. Since identical isocyanides are coordinated in both complexs, this difference illustrates the different capability for backbonding of the Re(III) units. The $[ReN(S^-)_3]$ moiety is much more electron-rich than the $[ReCl_3(PPh_3)_2]$ unit. The molecular parameters of the isocyanide ligands confirm this conclusion. Strong metal to ligand (d→p)π backbonding in **5b** leads to an isocyanide C–N–C angle of 154.0(10)° while the same angle in **4b**·CH_2Cl_2 has a value of 170.1(9)° (Table 12) which, like the wavenumber for the N≡C stretching vibration indicates,

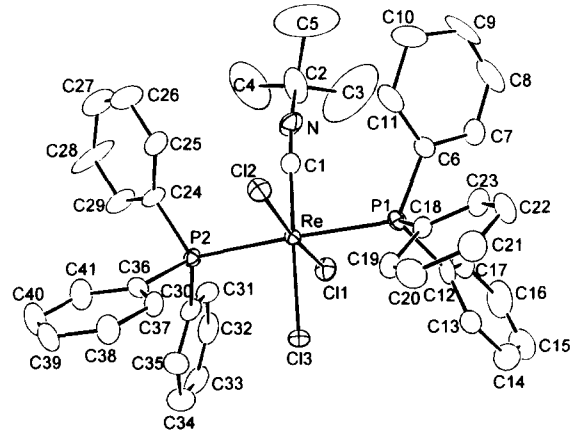

Fig. 4. Molecular structure of **4b** in **4b**·CH_2Cl_2.

Table 12
Selected bond distances (Å) and angels (°) for **4b**·CH_2Cl_2 [a]

Re–Cl1	2.338(2)
Re–Cl2	2.340(2)
Re–Cl3	2.426(2)
Re–P1	2.463(2)
Re–P2	2.468(2)
Re–C1	2.004(7)
P1–C6	1.832(7)
P1–C12	1.834(7)
P1–C18	1.825(6)
P2–C24	1.829(6)
P2–C30	1.839(7)
P2–C36	1.832(7)
N–C1	1.139(9)
N–C2	1.440(9)
C2–C3	1.50(2)
C2–C4	1.34(2)
C2–C5	1.56(2)
Cl1–Re–Cl2	173.15(6)
Cl1–Re–Cl3	89.56(6)
Cl1–Re–P1	88.28(6)
Cl1–Re–P2	91.09(6)
Cl1–Re–C1	82.6(2)
Cl2–Re–Cl3	97.03(5)
Cl2–Re–P1	89.98(6)
Cl2–Re–P2	90.92(6)
Cl2–Re–C1	90.8(2)
Cl3–Re–P1	89.09(6)
Cl3–Re–P2	88.47(5)
Cl3–Re–C1	172.1(2)
P1–Re–P2	177.49(5)
P1–Re–C1	91.5(2)
P2–Re–C1	90.8(2)
Re–P1–C6	114.4(2)
Re–P1–C12	114.8(2)
Re–P1–C18	118.8(2)
C6–P1–C12	106.6(3)
C6–P1–C18	99.6(3)
C12–P1–C18	100.6(3)
Re–P2–C24	115.6(2)
Re–P2–C30	112.3(2)
Re–P2–C36	117.6(2)
C24–P2–C30	104.8(3)
C24–P2–C36	101.5(3)
C30–P2–C36	103.5(3)
Re–C1–N	173.7(6)
C1–N–C2	170.1(9)

[a] E.s.d.s of the last significant figure are given in parentheses.

that the isocyanide in **4b**·CH_2Cl_2 acts mostly as σ-donor and receives almost no backbonding from the electron-poor Re(III) metal center. Inspite of the weak backbonding to the isocyanide carbon a small *trans*-effect is noticable for the Re–Cl3 bond (Table 12).

The isocyanide ligand in **4b**·CH_2Cl_2 must at least be bound as tightly to the rhenium center as all other ligands. Reaction of **4b**·CH_2Cl_2 with the tripodal, tetradentate ligand H_3**1** leads to substitution of all ligands, but the isocyanide and formation of the trigonal-bipyramidal complex **5b**. This reaction should be even more favored with isocyanides which are better π-acceptors and hence are tighter bound to rhenium. Thus complexes of type **4** are superb starting materials for substitution reactions starting with complexes of type **4** and leading to trigonal-bipyramidal complexes of type **5** in which the isocyanide ligand is retained. It should be noted, that the acetonitrile complex [$ReCl_3(PPh_3)_2$(NCMe)] shows a different reactivity towards substitution reactions. Nucleophiles will first substitute the acetonitrile ligand while in complexes of type **4** the isocyanide ligand is substituted last, if at all.

3.4. Reaction of isocyanide substituted rhenium complexes with acid and base

To investigate the possibility to couple rhenium complexes of type **5** over the isocyanide group to molecules with a specific biodistribution we studied reactions of complexes containing functionalized isocyanide ligands. For example, the ester groups in **5a** or **5e** could be used for coupling of the complex to a primary amine via formation of an amide bond. In addition, the neutral complexes **5a** and **5e** can be converted into an anionic derivative via ester hydrolysis and deprotonation of the carboxylic acid. Such behavior can influence the in vivo biodistribution of the complex. We studied therefore methods to hydrolyze the ester function in **5e**.

Reaction of **5e** in THF with LiOH/H_2O at room temperature results in ester hydrolysis and gives the lithium salt [Re(**1**)($CNCH_2COOLi$)], which was converted without isolation or purification into the isocyanacetic acid complex **6** by means of a cation-exchange resin (Scheme 6). The analytical and spectroscopic data for **6** (Table 2) are consistent with a trigonal-bipyramidal molecular structure as shown in Scheme 6.

The clean hydrolysis of the ester is surprising, since a nucleophile like OH^- can attack complex **5e** at two different sites: (i) at the ester group or (ii) at the isocyanide group. The latter attack is the standard reaction of coordinated isocyanides with nucleophiles and constitutes the oldest method for the synthesis of heteroatom-stabilized carbene complexes [23]. However, the attack at the isocyanide carbon atom is only possible for isocyanides which are not deactivated for nucleophilic attack by (d → p) π backbonding from the metal

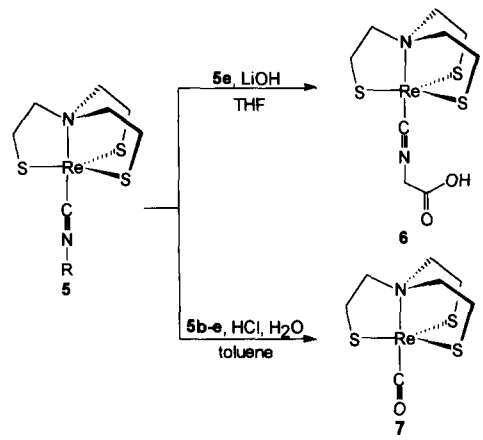

Scheme 6.

center [24]. As stated previously, strong backbonding to the isocyanide carbon atom was observed for all complexes of type **5**. This explains, why the isocyanide carbon was not attacked in the reaction of **5e** with LiOH, but instead the unusual ester hydrolysis was observed in the presence of an isocyanide function.

Even more surprising were the results when **5e** was treated with hydrochloric acid. After heating of **5e** in the two-phase system toluene/hydrochloric acid for 1 h, the original green color of the organic phase bleached and the water phase turned orange. Continued heating of the reaction mixture gave a lipophilic compound, which redissolved in the toluene phase, coloring this phase red. Standard workup of the toluene solution gave a deep red crystalline compound. The IR spectrum of this compound showed no absorptions which could be attributed to an isocyanide complex but instead a strong absorption was found at 1876 cm^{-1}. This suggested, that the carbonyl complex **7** (Scheme 6) had formed. An X-ray structure analysis with crystals of **7** confirmed this conclusion (Fig. 5). The asymmetric unit of crystalline **7** contains two, almost identical molecules. The rhenium atoms in these molecules are penta-coordinated by the tripodal ligand and one CO ligand in the axial position.

Formation of complex **7** was also observed upon treatment of the complexes **5b–5d** with hydrochloric acid. However, the yield of **7** was very low for reactions starting with **5c**. For the formation of **7** from complexes of type **5** we propose the mechanism depicted in Scheme 7. Due to the strong backbonding from the rhenium atom to the isocyanide carbon in complexes **5** (vide supra) these complexes are best represented by resonance formula B with a partly sp^2-hybridized isocyanide nitrogen atom. In the first reaction step (a) the isocyanide nitrogen atom is protonated, leading to the orange, water soluble species. In the water phase, the carbon atom of the protonated isocyanide is attacked by a water molecule (b) and HCl is eliminated. The resulting complex can be formulated as Re(II) derivative which can exist in two tautomeric forms C and D. Elimination of a primary amine (c) from D gives complex **7**. The poor yield in the reaction of **5c** can be attributed to the poor water solubility of protonated **5c**.

The observation of an electrophilic H^+ attack at the isocyanide nitrogen followed by a nucleophilic attack of OH^- at the carbon atom of the protonated isocyanide has not been reported yet. The only other reported conversion of a coor-

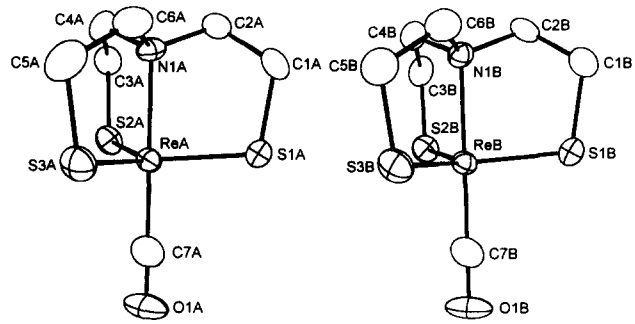

Fig. 5. Molecular structures of the two independent molecules in the asymmetric unit of **7**.

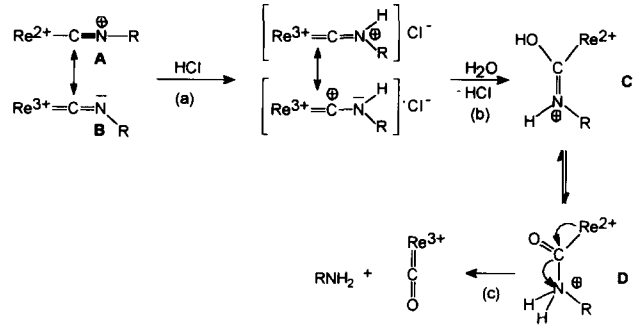

Scheme 7.

Table 13
Selected bond distances (Å) and angels (°) for **7** [a]

	molecule A	molecule B
Re–S1	2.226(2)	2.224(2)
Re–S2	2.243(2)	2.242(2)
Re–S3	2.241(2)	2.239(2)
Re–N1	2.227(5)	2.221(5)
Re–C7	1.888(7)	1.877(7)
S1–C1	1.816(7)	1.832(7)
S2–C3	1.819(7)	1.826(7)
S3–C5	1.846(8)	1.828(7)
O1–C7	1.152(9)	1.163(8)
N1–C2	1.483(8)	1.510(7)
N1–C4	1.488(8)	1.474(9)
N1–C6	1.500(9)	1.509(9)
C1–C2	1.500(9)	1.490(9)
C3–C4	1.491(10)	1.519(10)
C5–C6	1.483(11)	1.522(10)
S1–Re–S2	117.35(6)	117.35(7)
S1–Re–S3	120.27(7)	120.22(7)
S1–Re–N1	85.46(13)	86.08(13)
S1–Re–C7	94.4(2)	94.3(2)
S2–Re–S3	120.60(7)	120.69(6)
S2–Re–N1	85.45(14)	85.07(14)
S2–Re–C7	96.4(2)	96.3(2)
S3–Re–N1	85.79(14)	85.66(14)
S3–Re–C7	92.6(2)	92.7(2)
N1–Re–C7	178.0(2)	178.2(2)
Re–S1–C1	102.2(2)	102.4(2)
Re–S2–C3	101.8(2)	102.2(2)
Re–S3–C5	101.6(2)	102.8(2)
Re–N1–C2	109.6(3)	108.8(3)
Re–N1–C4	109.2(4)	110.3(4)
Re–N1–C6	108.5(4)	109.2(4)
C2–N1–C4	109.6(5)	110.7(5)
C2–N1–C6	109.8(5)	108.0(5)
C4–N1–C6	110.0(5)	109.9(5)
S1–C1–C2	111.5(4)	110.8(4)
N1–C2–C1	112.3(5)	113.3(5)
S2–C3–C4	112.4(5)	111.4(5)
N1–C4–C3	112.5(5)	111.6(5)
S3–C5–C6	110.6(5)	110.7(5)
N1–C6–C5	113.0(6)	112.1(5)
Re–C7–O1	178.8(6)	177.7(6)

[a] E.s.d.s of the last significant figure are given in parentheses.

dinated isocyanide ligand into a carbonyl is reported to proceed via nucleophilic attack at the carbon atom of a Pt(I) coordinated isocyanide followed by amine elimination [25]. As shown previously, hydroxyl ions cannot attack the isocyanide carbon atom in complexes of type **5**. Thus the first step in the reaction depicted in Scheme 6 must be an electrophilic attack at the isocyanide nitrogen atom. Protonation of Re(I) coordinated, electron-rich isocyanides by HBF_4 has been demonstrated by Pombeiro et al. [26]. Various other examples for the attack by H^+ or alkyl halides on electron-rich isocyanides have also been reported. These lead either to stable cationic carbyne type complexes [27] or, in case of protonation of the isocyanide, can rearrange to give metal hydrides [28]. A protonated isocyanide can be regarded as an iminocarbyne. Such ligands have been shown to be electron withdrawing [27a,d]. Thus the subsequent nucleophilic attack at the postulated iminocarbyne carbon by a water molecule (reaction b in Scheme 7), although not reported previously, becomes feasible. Finally it should be mentioned, that the $Re(NS_3)$ chelate unit remains unchanged in both base and acid catalyzed reactions at the isocyanides which is another testatment to the stability of this coordination type.

Crystals of **7** contain two, almost identical molecules (Table 13). Conversion of the isocyanide ligand into a carbonyl leaves the $Re(NS_3)$ unit virtually unchanged. The Re–CO bond is of course shorter than the Re–CNR bond in complexes of type **5**. However, no lengthening of the Re–N1 bond is observed.

4. Conclusions

The tripodal, tetradentate ligand H_3**1** reacts with $KTcO_4$ or NH_4ReO_4 in the presence of phosphines as reducing agents to give trigonal-bipyramidal complexes of the composition [M(**1**)(PR_3)] (M = Tc, Re). For the rhenium complexes we have shown, that the phosphine ligand can easily be substituted for an isocyanide ligand. The isocyanide ligand is tightly bound to Re(III). Strong backbonding from the electron-rich [Re(**1**)] fragment to the isocyanide carbon was observed. This backbonding leads in the case of ester substituted isocyanides to ester hydrolysis by hydroxyl ion, instead of nucleophilic attack at the isocyanide carbon atom. Hydrochloric acid reacts with complexes of the type [Re(**1**)(CNR)] under protonation of the electron-rich isocyanide nitrogen atom. Subsequent degradation reactions give the carbonyl complex [Re(**1**)(CO)].

5. Supplementary material

Tables of calculated positional parameters for the hydrogen atoms, all bond distances and angles, anisotropic temperature factors and calculated and observed structure factor amplitudes for crystallographically characterized compounds can be obtained from one of the authors (F.E.H.) on request.

Acknowledgements

We thank the Deutsche Forschungsgemeinschaft and the Fonds der Chemischen Industrie e.V. for financial support of our work. Dr D. Scheller is acknowledged for measuring some of the NMR spectra.

References

[1] P.J. Blower, J.R. Dilworth, J.P. Hutchinson, T. Nicholson and J. Zubieta, *J. Chem. Soc., Dalton Trans.*, (1986) 1339.
[2] (a) N. de Vries, A. Davison and A.G. Jones, *Inorg. Chim. Acta, 165* (1989) 9; (b) N. de Vries, J. Cook, A.G. Jones and A. Davison, *Inorg. Chem., 30* (1991) 2662; (c) T. Nicholson, J. Cook, A. Davison and A.G. Jones, *Inorg. Chim. Acta, 218* (1994) 97.
[3] S.G. Mastrostamatis, M.S. Papadopoulos, I.C. Pirmettis, E. Paschali, A.D. Varvarigou, C.I. Stassinopoulou, C.P. Raptopoulou, A. Terzis and E. Chiotellis, *J. Med. Chem., 37* (1994) 3212.
[4] (a) H. Spies, M. Glaser, H.-J. Pietzsch, F.E. Hahn, O. Kintzel and T. Lügger, *Angew. Chem., Int. Ed. Engl., 33* (1994) 1354; (b) M. Glaser, H. Spies, T. Lügger and F.E. Hahn, *J. Organomet. Chem.*, in press.
[5] S. Jurisson, D. Berning, W. Jia and D. Ma, *Chem. Rev., 93* (1993) 1137.
[6] J. Burgess, *Transition Met. Chem., 18* (1993) 439.
[7] P. Koch and H.R. Mäcke, *Angew. Chem., Int. Ed. Engl., 31* (1992) 1507.
[8] R. Obrecht, R. Herrmann and I. Ugi, *Synthesis*, (1985) 400.
[9] J. Chatt and G.A. Rowe, *J. Chem. Soc.*, (1962) 4019.
[10] G. Rouschias and G. Wilkinson, *J. Chem. Soc. A*, (1967) 993.
[11] R.M. Pearlstein, W.M. Davis, A.G. Jones and A. Davison, *Inorg. Chem., 28*, (1989) 3332.
[12] H. Spies, M. Glaser, F.E. Hahn, T. Lügger and D. Scheller, *Inorg. Chim. Acta, 232* (1995) 235.
[13] M. Veith and H. Bärnighausen, *Acta Crystallogr., Sect. B, 30* (1974) 1806.
[14] *MolEN*, Molecular Structure Solution Procedures, Program Description, Delft Instruments, Holland, 1990.
[15] N. Walker and D. Stuart, *Acta Crystallogr., Sect. A., 39* (1983) 158.
[16] M.R. Churchill, *Inorg. Chem., 12* (1973) 1213.
[17] D.T. Cromer and J.B. Waber, *International Tables for X-ray Crystallography*, Vol. IV, Kynoch, Birmingham, UK, 1974, Table 2.2B.
[18] D.T. Cromer, *International Tables for X-ray Crystallography*, Vol. IV, Kynoch, Birmingham, UK, 1974, Table 2.3.1.
[19] (a) J.Y. Gauthier, F. Burdon and R.N. Young, *Tetrahedron Lett., 27* (1986) 15; (b) P.A. Bobbio, *J. Org. Chem., 26* (1961) 3023.
[20] R.D. Shannon, *Acta Crystallogr., Sect. A, 32* (1976) 751.
[21] (a) J.-M. Bassett, D.E. Berry, G.K. Barker, M. Green, J.A.K. Howard and F.G.A. Stone, *J. Chem. Soc., Dalton Trans.*, (1979) 1003; (b) M.F.N.N. Carvalho, M.T. Duarte, A.M. Galvao and A.J.L. Pombeiro, *J. Organomet. Chem., 469* (1994) 79.
[22] (a) E.W. Randall and D. Shaw, *J. Chem. Soc. A*, (1969) 2867; (b) H.P. Gunz and G.J. Leigh, *J. Chem. Soc. A*, (1971) 2229.
[23] L. Tschugajeff, M. Skanawy-Grigorjewa and A. Posnjack, *Z. Anorg. Allg. Chem., 148* (1925), 37.
[24] (a) K.H. Dötz, H. Fischer, P. Hofmann, F.R. Kreissl, U. Schubert and K. Weiss, *Transition Metal Carbene Complexes*, VCH, Weinheim, 1983; (b) B. Crociani, in P.S. Braterman (ed.), *Reactions of Coordinated Ligands*, Vol. 1, Plenum Press, New York, 1985; (c) J. Chatt, R.L. Richards and G.H.D. Royston, *J. Chem. Soc., Dalton. Trans.*, (1973) 1433.
[25] B. Crociani, F. Di Bianca, A. Fontana, E. Forsellini and G. Bombieri, *J. Chem. Soc., Dalton Trans.*, (1994) 407.

[26] A.J.L. Pombeiro, M.F.N.N. Carvalho, P.B. Hitchcock and R.L. Richards *J. Chem. Soc., Dalton Trans.*, (1981) 1629.

[27] (a) J. Chatt, A.J.L. Pombeiro and R.L. Richards, *J. Chem. Soc., Dalton. Trans.*, (1980) 492; (b) J. Chatt, A.J.L. Pombeiro, R.L. Richards, G.H.D. Royston, K.W. Muir and R. Walker, *J. Chem. Soc., Chem. Commun.*, (1975) 708; (c) S. Willis, A.R. Manning and F.S. Stephens, *J. Chem. Soc., Dalton Trans.*, (1980) 186; (d) M. Amelia, N.D.A. Lemos and A.J.L. Pombeiro, *J. Organomet. Chem., 356* (1988) C79.

[28] J. Chatt, A.J.L. Pombeiro and R.L. Richards, *J. Chem. Soc., Dalton. Trans.*, (1979) 1585.